Low Power Beamforming for Underwater Acoustic Sensing Using a 5-Element Circular Hydrophone Array

Graham McIntyre*, Chris Loadman†, Jean-François Bousquet* and Stephane Blouin‡
*Department of Electrical and Computer Engineering,
Dalhousie University, Halifax, Nova Scotia
†Turbulent Research, Dartmouth, Nova Scotia
‡DRDC Atlantic Research Centre, Dartmouth, Nova Scotia

***Abstract*—In this paper we present a technique for underwater acoustic beamforming based on soundfield recording that encodes both the temporal and spatial characteristics of a signal. Here, we introduce the basic theory behind soundfield recording and present a first-order beamformer that beamforms the encoded data in a specific direction (θ, ϕ) and with a variable polar pattern, p. The appeal of this beamformer being that a 2-dimensional beam can be created using only 4 multiplications and 2 additions.**

A method for implementing a wideband, planar soundfield recorder using a 5-element array is then discussed. Results from underwater experimental trials using this 5-element array are then presented that compare the measured beam patterns and frequency response of the physical beamformer to the ideal, theoretical beam patterns and frequency response.

I. Introduction

Underwater acoustic monitoring has many applications ranging from passive acoustic sensing to detect and track marine mammals to wideband underwater acoustic communication to transmit high bandwidth data. While the applications are quite different, they suffer from many of the same problems.

In high-flow environments turbulent flow around hydrophones couples to acoustic measurements as noise and can increase the noise floor by upwards of 40 dB [1]. Multipath propagation causes multiple instances of the same signal that arrive from different directions and at different times causing delay spread. And lastly, many underwater signals of interest are broadband, or impulsive in nature and so the devices used to record such signals need to be broadband as well.

One method that can be used to address these problems is wideband beamforming. However, this is not readily implemented in small underwater sensors due to the complexity and power consumption that generally accompanies broadband spatial filtering.

In this paper we present a low-power, low-complexity real-time beamforming technique that uses a small, 5-element circular hydrophone array. This technique makes use of soundfield recording techniques in order to provide directionality to the recorded signal as well as to reduce the noise introduced by uncorrelated flow noise around the hydrophones in the array.

The paper is broken down as follows. In Section II the basics of soundfield recording are reviewed and the algorithms required to produce a soundfield beamformer are derived. In Section III practical issues with implementing this beamformer in an underwater environment are discussed, and a compensating filter is introduced that allows for wideband, planar soundfield recordings using a 5-element array. Lastly, section IV compares the theoretical performance of the beamformer to results obtained during underwater trials that were conducted.

II. Soundfield Recording

A soundfield is a region in space where acoustic waves propagate that vary with time and space, and so both temporal and directional information can be recorded for a signal. A sounfield can be recorded using spherical harmonic decomposition. Where spherical harmonics are a set of orthogonal basis functions that are used to encode a function that exists on the surface of a sphere into a series representation. Theoretically, if the number of basis functions used is infinite then the soundfield can be recreated perfectly. In reality, the series is generally truncated to a specific order, n, because it limits the number of channels that need to be recorded.

For the n^{th} order in the series there are $2n+1$ linearly independent harmonics that exist. The total number of harmonics required to produce an m^{th} order recording, including orders 0 to m, is [2]

$$\mathrm{N}_{\text{Harmonics}} = \sum_{n=0}^{m}(2n+1) = (n+1)^2. \tag{1}$$

Even for a second order recording this involves recording 9 channels simultaneously.

Practical sounfield recording techniques are therefore often limited to first or second order schemes. While a number of different first and second order basis functions can be used, there is a canonical set that is described using Legendre's polynomials and Legendre's associated functions [3].

$$\mathrm{P}_n(\sin\phi) \tag{2a}$$
$$\cos(m\theta)\mathrm{P}_n^m(\sin\phi) \quad 1 \le m \le n \tag{2b}$$
$$\sin(m\theta)\mathrm{P}_n^m(\sin\phi) \quad 1 \le m \le n \tag{2c}$$

These functions are described in spherical coordinates in accordance with most audio engineering literature [3]. θ is the azimuthal angle measured counter clockwise off the x-axis and ϕ is the polar angle zeroed on the x-y plane. ϕ is positive for angles of elevation and negative for angles of depression.

In (2), P_n represents a Legendre polynomial of order n and P_n^m represents the associated Legendre's function of the first

TABLE I: Spherical Harmonic basis functions up to order 2.

n	**m**	Spherical Harmonic	Channel Name
0	0	1	W
1	0	$\sin(\phi)$	Z
1	1	$\cos(\theta)\cos(\phi)$	X
		$\sin(\theta)\cos(\phi)$	Y
2	0	$\frac{1}{4}(1-3\cos(2\phi))$	R
2	1	$\frac{3}{2}\cos(\theta)\sin(2\phi)$	S
		$\frac{3}{2}\sin(\theta)\sin(2\phi)$	T
2	2	$2\cos(2\theta)\cos^2(\phi)$	U
		$2\sin(2\theta)\cos^2(\phi)$	V

kind of degree m and order n [3], [4]. Again, order and degree are chosen to comply with audio engineering conventions although the meanings are often reversed in mathematical literature. Using these formulas, the harmonics required for zeroth, first and second degree recordings can be calculated in spherical coordinates and are displayed in Table 1, along with their associated audio recording channel names.

Using these harmonics, a function, $f(\bar{\theta},\bar{\phi})$, impinging on the unit sphere from a direction, $(\bar{\theta},\bar{\phi})$, can now be represented using a weighted series of spherical harmonics [3]. This approximation is written as

$$f(\bar{\theta},\bar{\phi}) = \sum_{\mathrm{n}=0}^{\infty} A_{\mathrm{n}}\mathrm{P}_{\mathrm{n}}(\sin\bar{\phi}) + \sum_{\mathrm{n}=1}^{\infty}\sum_{\mathrm{m}=1}^{\mathrm{n}}(A_{\mathrm{n,m}}\cos(\mathrm{m}\bar{\theta}) + B_{\mathrm{n,m}}\sin(\mathrm{m}\bar{\theta}))\mathrm{P}_{\mathrm{n}}^{\mathrm{m}}(\sin(\bar{\phi})), \quad (3)$$

where A_{n}, $A_{\mathrm{n,m}}$, and $B_{\mathrm{n,m}}$ are weighting coefficients. The formulae to compute these are excluded here, but can be found in [3], [4].

The relationship between spherical harmonics and acoustic recording is best understood by plotting the harmonics. Figure 1 shows plots of the zeroth, first and second order harmonics on the first, second and third rows of the plot, respectively.

The polar patterns in Figure 1 indicate that the zeroth order harmonic is simply a recording device with an omnidirectional pattern while the first order harmonics are recording devices with figure-eight patterns oriented along the x, y and z axes. A popular sounfield recording technique called Ambisonics makes use of just the zeroth and first order harmonics to record what is known as a B-format signal. The focus of this paper is on first order recordings, and because of this the rest of the paper will deal only with the zeroth and first order recordings, or the B-format signals.

An omnidirectional recorder is simply a device that measures the sound pressure at a given point in space regardless of direction. A figure-eight pattern is harder to produce as it weights angles of arrival differently. One method for producing a figure-eight pattern is using a spatial derivative, which is commonly referred to as a pressure gradient recorder. To show that this does in fact produce the desired figure-eight harmonics, a simple derivation can be used which uses the directional derivative of a signal traveling through space [3].

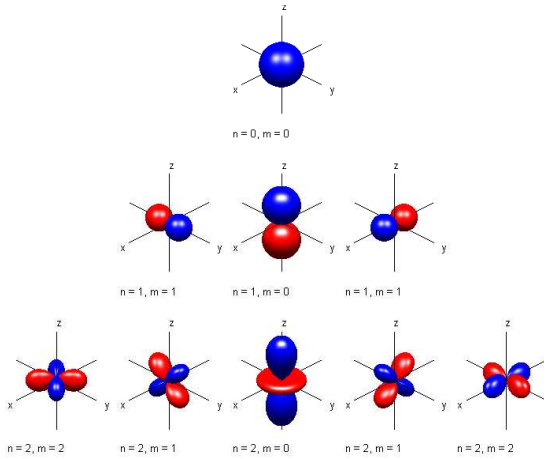

Fig. 1: Plot of zeroth, first and second order spherical harmonics. Blue indicates in phase recordings, red indicates out of phase recordings or recordings phase shifted by π.

If the signal of interest has a frequency, ω, wavenumber, k, and amplitude, A, then it can be represented as a function of time, t, and space, $\mathbf{x}$, as

$$p(t,\mathbf{x}) = Ae^{j(\omega t+\mathbf{kx})}. \quad (4)$$

Here, $\mathbf{k}$ is the wave vector that indicates the direction of incidence of the received wave. If the wave is arriving from $(\bar{\theta},\bar{\phi})$, then the wave vector is

$$\mathbf{k} = k\begin{bmatrix}\cos(\bar{\theta})\cos(\bar{\phi})\\ \sin(\bar{\theta})\cos(\bar{\phi})\\ \sin(\bar{\phi})\end{bmatrix}. \quad (5)$$

If the recording occurs at $\mathbf{x}=\mathbf{0}$, and at a single instant in time, t, then $p(t,\mathbf{x})$ can be replaced with p. With this simplification, the spatial derivative of the signal can be shown to be

$$\nabla p = jk\begin{bmatrix}\cos(\bar{\theta})\cos(\bar{\phi})\\ \sin(\bar{\theta})\cos(\bar{\phi})\\ \sin(\bar{\phi})\end{bmatrix}p. \quad (6)$$

In order to determine the derivative along a specific direction, ∇p can be projected onto a unit vector pointing in the direction of interest, $(\hat{\theta},\hat{\phi})$. The dot product of $\mathbf{u}_1$ and ∇p yields the scalar directional derivative of the incident wave with respect to the direction of $\mathbf{u}_1$.

$$\begin{aligned}\mathbf{u}_1\cdot\nabla p &= \begin{bmatrix}\cos(\hat{\theta})\cos(\hat{\phi})\\ \sin(\hat{\theta})\cos(\hat{\phi})\\ \sin(\hat{\phi})\end{bmatrix}\cdot jk\begin{bmatrix}\cos(\bar{\theta})\cos(\bar{\phi})\\ \sin(\bar{\theta})\cos(\bar{\phi})\\ \sin(\bar{\phi})\end{bmatrix}p\\ &= jk[\cos(\hat{\phi})\cos(\bar{\phi})\cos(\bar{\theta}-\hat{\theta})\\ &\quad +\sin(\hat{\phi})\sin(\bar{\phi})]p \end{aligned} \quad (7)$$

If the unit vector is chosen to be along the x-axis ($\hat{\theta}=0,\hat{\phi}=0$), then the projection becomes,

$$\mathbf{u}_x\cdot\nabla p = jk[\cos(\bar{\phi})\cos(\bar{\theta})]p. \quad (8)$$

This is the original signal, p, multiplied by the first-order spherical harmonic along the x-axis. The main difference is

that this signal has been multiplied by j, or shifted by $\frac{\pi}{2}$, and scaled by k. A method for removing both the phase shift and scaling will be discussed in section III.

Similarly, if $\hat{\theta}$ and $\hat{\phi}$ are chosen to point along the y-axes, $(\hat{\theta} = \frac{\pi}{2}, \hat{\phi} = 0)$, and z-axis, $(\hat{\theta} = 0, \hat{\phi} = \frac{\pi}{2})$, then the resulting signal outputs are the original signal, p, weighted by the first-order harmonics in the y and z directions, respectively.

With the link between zeroth and first-order harmonics to omnidirectional and pressure-gradient recorders, respectively, the focus shifts towards a method to decode these signals to produce a beamformed output. To do this, a linear combination of the signals can be taken. However, in a first-order recording there are 4 recorded signals and there are only two desired constraints, direction and pattern. So in order to create a beamformed output two additional constraints are required.

By combining the first-order harmonics such that they produce a single figure-eight pattern pointing in a desired direction, (θ, ϕ), two new constraints are created. To do this the x-axis, which is considered the zero position, $(\theta = 0, \phi = 0)$, can be rotated around the z-axis by θ, and then it can be rotated around the y-axis by ϕ. The new resulting coordinate system from the consecutive rotations can be expressed as

$$\begin{aligned}\hat{\mathbf{X}} &= \mathbf{R}_y \mathbf{R}_z \mathbf{X} \\ &= \begin{bmatrix} \cos(\phi) & 0 & -\sin(\phi) \\ 0 & 1 & 0 \\ \sin(\phi) & 0 & \cos(\phi) \end{bmatrix} \begin{bmatrix} \cos(\theta) & \sin(\theta) & 0 \\ \sin(\theta) & \cos(\theta) & 0 \\ 0 & 0 & 1 \end{bmatrix} \mathbf{X}. \end{aligned} \quad (9)$$

Where $\hat{\mathbf{X}}$ represents the rotated first-order harmonics and $\mathbf{X}$ represents the original first-order harmonics. Since $\hat{X}$ is the only new first-order pattern of interest pointing in the desired direction, both $\hat{Y}$ and $\hat{Z}$ can be discarded and the new rotated figure-eight pattern can be written as

$$\hat{\mathrm{X}} = \cos(\theta)\cos(\phi)\mathrm{X} + \sin(\theta)\cos(\phi)\mathrm{Y} + \sin(\phi)\mathrm{Z}, \quad (10)$$

where X, Y and Z represent the spherical harmonics recorded in the x, y, and z directions, respectively.

The rotated harmonic, $\hat{\mathrm{X}}$, can now be combined with the output of the omnidirectional recorder, W, to produce the beamformed output, M.

$$\begin{aligned}\mathrm{M}(a, b, \theta, \phi) &= a\mathrm{W} + b\hat{\mathrm{X}} \\ &= a\mathrm{W} + b[\cos(\theta)\cos(\phi)\mathrm{X} \\ &\quad + \sin(\theta)\cos(\phi)\mathrm{Y} + \sin(\phi)\mathrm{Z}] \end{aligned} \quad (11)$$

The beamformed output are generally normalized such that along the axis of interest, $\hat{\mathrm{X}}$, the gain is unitary with respect to the omnidirectional recording. This leads to

$$a + b = 1 \quad \rightarrow \quad b = 1 - a. \quad (12)$$

Often, instead of using a, the pattern is described using a patterm parameter, p, that defines both a and b. With p defined, the final beamforming equation becomes

$$\begin{aligned}\mathrm{M}(p, \theta, \phi) &= p\mathrm{W} + (p-1)[\cos(\theta)\cos(\phi)\mathrm{X} \\ &\quad + \sin(\theta)\cos(\phi)\mathrm{Y} + \sin(\phi)\mathrm{Z}]. \end{aligned} \quad (13)$$

In this paper height information is not considered. Instead, the focus is on the 2-dimensional X-Y plane. With this simplification the polar angle is considered to always be zero, $\phi = 0$, and the beamforming equation in the X-Y plane becomes

$$\mathrm{M}(p, \theta) = p\mathrm{W} + (p-1)[\cos(\theta)\mathrm{X} + \sin(\theta)\mathrm{Y}]. \quad (14)$$

Eqn. 14 appears frequently in recording literature using soundifeld decomposition to describe a 'virtual microphone' pattern [5], [6], [7].

The zeroth and first-order circular harmonics required for a 2-dimensional soundfield recording in the X-Y plane are shown in Figure 2.

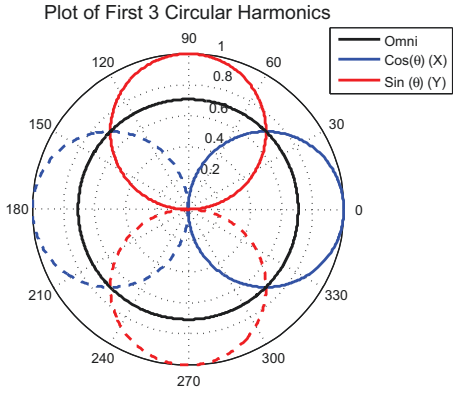

Fig. 2: Zeroth and first order circular harmonics. Dashed line indicates phase shift of π.

Figure 2 shows that for the planar case only three signals are required for 2-dimensional soundfield recording. The channels correspond to an omnidirectional recorder, a cosine figure-eight recorder pointed along $\theta = 0$ and a sine figure-eight recorder pointed along $\theta = \frac{\pi}{2}$. These signals are referred to as the omni, cosine and sine channels, respectively.

Figure 3 shows plots of different theoretical beamformer patterns attained by changing the pattern parameter, p, and the steering angle, θ.

The first-order beamformer in Eqn. 14 does not provide extremely small beamwidths, as shown in Figure 3. However, as the order of the system is increased, the possible beamwidths become much narrower. The true benefit of this beamforming method is that once the omni, cosine and sine channels are created a beam can be implemented using only 4 multiplications and two additions. So the computational cost of creating a large number of beams is extremely low.

III. Underwater Soundfield Recording

In order for soundfield recording to be viable for underwater beamforming, it also needs to be wideband and easily implementable. To implement a 2-dimensional, or planar, soundfield recorder the 5-element circular hydrophone layout shown in Figure 4 was used. It should be noted that hydrophone replaces the use of recorder in this section to indicate the recording occurs underwater.

To produce a first-order planar soundfield recording an omni, cosine, and sine channel need to be recorded. An extra constraint is that these signals also need to be recorded coincidentally, or in the same spatial position, **x**, and at the same time, t. Deviations in either position or timing cause phase errors between the recorded channels.

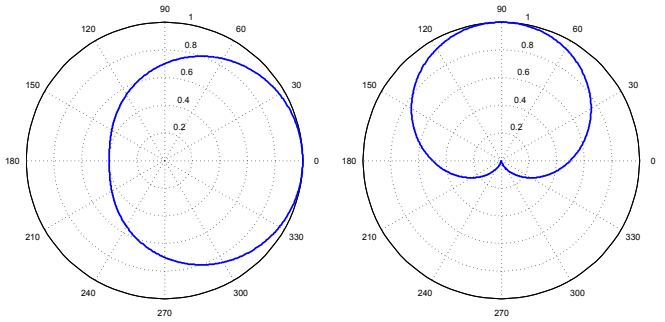

(a) p=0.7, $\theta = 0$ (b) p=0.5, $\theta = 90$

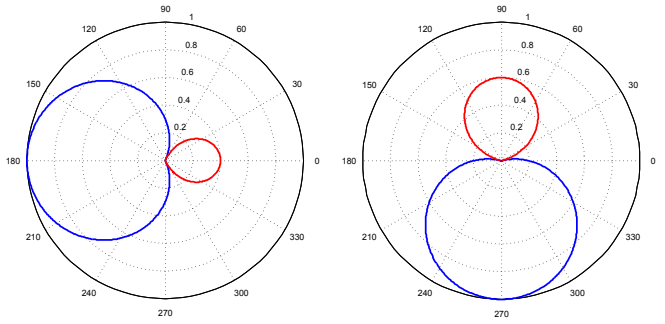

(c) p=0.3, $\theta = 180$ (d) p=0.2, $\theta = 270$

Fig. 3: Polar patterns of the beamformer for different pattern values, p, and azimuthal angles, θ. Blue indicates in phase, red indicates out of phase or shifted by π.

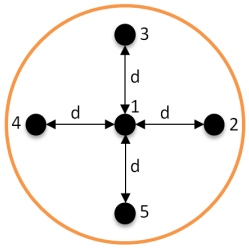

Fig. 4: 5-element array configuration. Each hydrophone is numbered and d is the spacing from the central hydrophone.

Hydrophone 1 in Figure 4 was chosen as the reference recording position in this work, or $\mathbf{x} = \mathbf{0}$. The omni channel was therefore recorded using hydrophone 1 and the directional cosine and sine channels were created using the Blumlein difference technique with the remaining hydrophones [3], [8]. This technique states that two hydrophones of order n can be used to produce an output of order n+1. In this case, two pressure hydrophones of order 0 were used to produce the desired first-order harmonic.

A first-order pattern can be produced using the derivative of a signal projected onto the axis of interest, as shown in Section II. The use of discrete hydrophones means a finite difference scheme can be used to approximate the derivative. To satisfy the requirement that the output of the first-order channel be coincident with the omni channel, a central difference formula was applied. The approximation of the derivative using the pressure wave from Eqn. 4 is then

$$\begin{aligned}\nabla p(t,\mathbf{x}) &\approx p(t,\mathbf{x}+\mathbf{d}) - p(t,\mathbf{x}-\mathbf{d}) \\ &= Ae^{j(\omega t+\mathbf{k}(\mathbf{x}+\mathbf{d})} - Ae^{j(\omega t+\mathbf{k}(\mathbf{x}+\mathbf{d})} \\ &= j2p(t,\mathbf{x})\sin(\mathbf{kd}). \end{aligned} \tag{15}$$

Here, we assume that the elements used for the differencing are negative symmetric in spacing, and only act along one axis. This means only pairs 2,4 and 3,5 can be used to produce the first-order channels. With these assumptions, the directional derivative is simplified. With hydrophones at $-d$ and $+d$ on the x-axis, the derivative along the x-axis can then be written as

$$\begin{aligned}\mathbf{u}_x \cdot \nabla p(t,\mathbf{x}) &\approx j2p(t,\mathbf{x})\sin\left(k\begin{bmatrix}\cos(\bar{\theta})\\ \sin(\bar{\theta})\end{bmatrix}\cdot d\begin{bmatrix}1\\0\end{bmatrix}\right) \\ &= j2p(t,\mathbf{x})\sin\left(kd\cos(\bar{\theta})\right) \\ &= j2p(t,\mathbf{x})\sin\left(\frac{2\pi f}{c}d\cos(\bar{\theta})\right). \end{aligned} \tag{16}$$

Similarly, if the y-axis is chosen as the axis of interest and the hydrophones are located at $-d$ and $+d$ on the y-axis, then the directional derivative is

$$\mathbf{u}_y \cdot \nabla p(t,\mathbf{x}) \approx j2p(t,\mathbf{x})\sin\left(\frac{2\pi f}{c}d\sin(\bar{\theta})\right). \tag{17}$$

The choice of hydrophone pair used for the cosine channel is arbitrary and simply sets the position of the x-axis along the line connecting the hydrophones in the pair. The choice of which hydrophone in the pair is at $+d$ and $-d$ sets the reference for where $\theta = 0$ and $\theta = \pi$, respectively. The remaining pair can then be used for the sine channel, with the hydrophones at $+d$ and $-d$ setting the reference for where $\theta = \frac{\pi}{2}$ and $\theta = \frac{3\pi}{2}$, respectively.

Using the central difference approximation for the directional derivative of the signal presents two problems. First, as shown in Section II, the derivative causes the first order outputs to lead the omni channel by $\frac{\pi}{2}$. Second, the use of the approximation leads to a frequency dependent gain term. To resolve these problems a compensating filter can be designed that implements a frequency independent phase delay of $\frac{\pi}{2}$ and that compensates for the frequency dependent gain.

To remove the constant phase shift a Hilbert transform of the signal can be used. The Hilbert transform of a signal multiplies the positive frequencies by $-j$, causing a phase shift of $-\frac{\pi}{2}$, and multiplies the negative frequencies by j, causing a further phase shift of $\frac{\pi}{2}$. The Fourier transform of the Hilbert transform is [9]

$$H_H(f) = \begin{cases} -j, & f \geq 0 \\ j, & f < 0 \end{cases} \tag{18}$$

To mitigate the frequency dependent gain in Eqn. 16 and 17 caused by the directional derivative, an inverse filter can be designed. The desired response along the x-axis uses Eqn. 16 with $\bar{\theta} = 0$ and along the y-axis the desired response is found

using Eqn. 17 with $\bar{\theta} = \frac{\pi}{2}$. In both cases the required inverse filter is

$$H_I(f) = \frac{1}{\sin\left(\frac{2\pi f}{c} d\right)}, \tag{19}$$

where c is the speed of acoustic propagation in the medium.

Similar compensating filters for the output of first-order differencing schemes are presented in [6], [7].

The exact procedure to design these filters is not discussed in this paper as there are a number of filter design techniques that can be used. Once both filters are designed, the first-order channel filter, $H_{FO}(f)$, is created by convolving the two filters together.

$$H_{FO}(f) = H_I(f) * H_H(f) \tag{20}$$

The resulting first-order filter can then be applied to the output of the difference of either pairs of hydrophones to produce a frequency-flat, first-order channel that is coincident with the omni hydrophone.

A characteristic of interest for the beamformer is its functional bandwidth. This depends on both the layout of the hydrophones and the design of the first-order filter. To determine this bandwidth, the maximum and minimum frequencies where the beamformer functions as desired need to be determined.

The maximum frequency of the beamformer is set by the spacing of the discrete elements used to create the first order channels. To avoid spatial aliasing, the maximum frequency is

$$f_{max} = \frac{c}{4d}. \tag{21}$$

The minimum frequency is set by the lower passband limit of the first-order filter. If the the first-order filter has a passband from a normalized frequency of ω_l to ω_u, then the minimum frequency can be expressed using ω_l and the sampling frequency, f_s.

$$f_{min} = \omega_l \frac{f_s}{2} \tag{22}$$

The bandwidth of the beamformer is then

$$BW_{BF} = f_{max} - f_{min} = \frac{c}{4d} - \omega_l \frac{f_s}{2} \tag{23}$$

The sampling frequency can be chosen to maximize the functional bandwidth. To do this, the upper passband limit, $\omega_u \frac{f_s}{2}$, should be equal to the maximum frequency allowed by the spacing of the elements, f_{max}. This can be written using the inequality

$$\omega_u \frac{f_s}{2} \geq f_{max} \quad \rightarrow \quad f_s \geq \frac{2 f_{max}}{\omega_u}. \tag{24}$$

If f_s is chosen to satisfy the equality in Eqn. 24, then the maximum bandwidth simply becomes the bandwidth, or passband, of the first-order filter.

$$BW_{max} = f_{max} - f_{min} = (\omega_u - \omega_l)\frac{f_s}{2}. \tag{25}$$

If f_s is chosen to be greater than the critical sampling frequency, the passband of the first order filter is not fully utilized. This critical bandwidth stresses the importance of a first-order filter design that provides an accurate, and large passband in order to have a broadband beamformer.

A finite impulse response (FIR) first-order filter was designed for the experimental apparatus described in Section IV with $d = 0.0381$ m and using a speed of propagation in fresh water of $c = 1476$ m/s. The lower and upper limits of the passband on this filter were $\omega_l = 0.04$ and $\omega_u = 0.96$, respectively. With this filter, and a sampling frequency of $f_s = 20$ kHz the bandwidth of the beamformer was 9.44 kHz with a maximum frequency of $f_{max} = 9.84$ kHz and $f_{min} = 0.4$ kHz.

Figures 5a and 5b show simulations of the directional and frequency response of the beamformer with this first-order filter applied when $p = 0.5$ and $p = 0.3$, respectively, with $\theta = 0$.

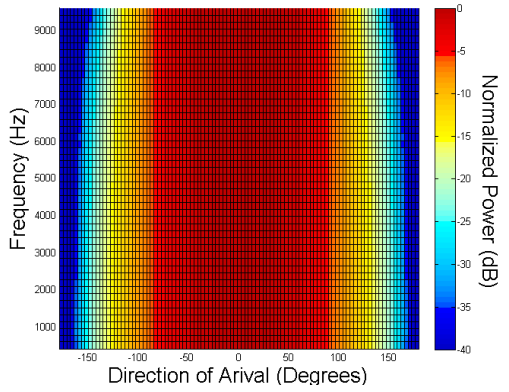

(a) $p = 0.5$

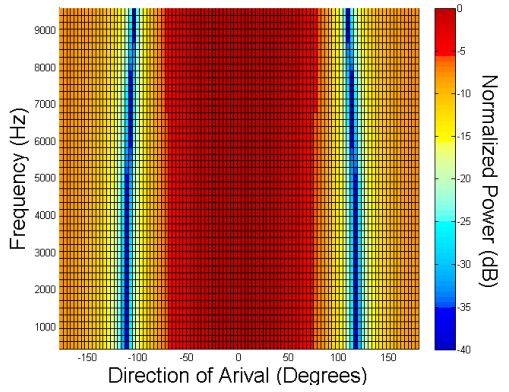

(b) $p = 0.3$

Fig. 5: Simulated polar plots with respect to direction of arrival, θ, and frequency, f.

One major issue with the use of the first-order filter is the frequency dependent gain that is applied to uncorrelated noise sources on the hydrophones, such as flow noise. While the first order filter ensures the output of the hydrophone differencing is frequency flat for correlated signals, if there is uncorrelated noise present then this filter simply applies gain to the noise.

The critical uncorrelated noise frequency, f_{Crit}, is used to describe the frequency where the noise floor at the output of the beamformer switches from being attenuated, to being

amplified. This equation is related to the pattern parameter, p, and assumes the same noise power, and spectral shape at each hydrophone.

$$f_{Crit} = \frac{c}{2\pi d} \sin^{-1}\left(\sqrt{\frac{(1-p)^2}{2(1-p^2)}}\right) \tag{26}$$

In deployments with high, uncorrelated noise powers, such as in an environment with high flow, the lower frequency in the functional bandwidth might therefore be set by the frequency at which the noise is actually amplified versus attenuated, f_{Crit}. Future experiments are planned to explore these effects further.

As was mentioned at the beginning of this section, one of the benefits of using a soundfield recording technique for beamforming is the ease with which multiple beams can be created and how few filters need to be implemented in order to maintain a frequency flat output. Figure 6 demonstrates that only one delay line, accounting for the group delay of $H_{FO}(f)$, and two first-order filters are required in order to create the omni, cosine and sine outputs required to produce any beam.

Forming an actual beam requires only 4 multiplications and 2 additions, and so implementing multiple beams is extremely computationally efficient. Most wideband beamforming techniques require space-time filters applied to each hydrophone in order to get similar results [10], and for each beam, different filters would need to be applied making it very difficult to have multiple beams steered in real time and with low power consumption.

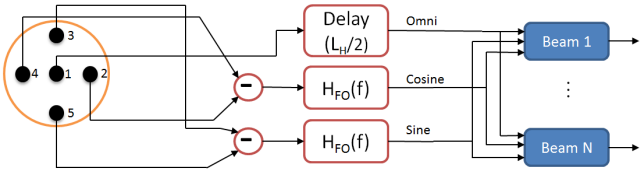

Fig. 6: Flow of data from hydrophones to beamformer 1 to N outputs.

IV. Experimental Results

In order to verify the theory presented above, experimental underwater trials were conducted. The 5-element hydrophone array was mounted onto the end cap of the TR-Orca, which is an autonomous underwater data acquisition system. This platform was provided by Turbulent Research. The spacing between the elements in this array is 0.0381 m. The TR-Orca was used to record the 5-channels required to implement the planar soundfield recording.

The experiment was carried out in the anechoic tank at Defence Research and Development Canada Atlantic (DRDC). This tank is cylindrical in shape with a 7.3 m diameter and with a depth of 4.5 m. DRDC Atlantic also provided a broadband piston-actuated acoustic source and the equipment required to drive it. A side view of the experimental deployment is shown in Figure 7 and a bottom view of the experimental deployment is shown in Figure 8.

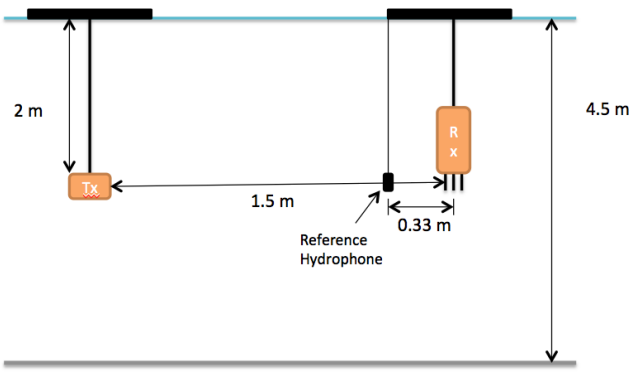

Fig. 7: Side view of the experimental deployment.

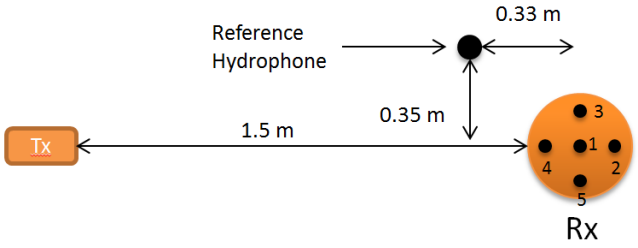

Fig. 8: Bottom view of the experimental deployment.

The transmitter, Tx, (the piston actuated source) and the 5-element receiver, Rx, (the TR-Orca) were both placed at a depth of 2 m in order to maximize the time between the direct path arrival and the multipath arrival. Both the receiver and transmitter were placed at the same depth to ensure that this was a test of the planar directionality and that no height information would effect the recorded data. The transmitter and receiver were placed 1.5 meters apart so that far field conditions were met.

The bottom view in Figure 8 shows the orientation of the hydrophones, which allows the proper hydrophones to be used to create the cosine and sine channels. Specifically, for this experiment hydrophone 4 was subtracted from hydrophone 2 to create the cosine channel, with $\theta = 0$ on the line from hydrophone 1 to 4. Hydrophone 5 was subtracted from hydrophone 3 to create the sine channel, and $\theta = \frac{\pi}{2}$ was on the line from hydrophone 1 to 5. The first-order filter described in Section III was applied to the output of these filters in order to create frequency-flat first-order outputs from 0.4 to 9.44 kHz.

The receiver was connected to an actuator that could rotate it. The actuator controller was zeroed at the position shown in Figure 8. During post-processing it was found that the zeroed position was off by about -11° degrees, and so the direction of all of the recorded data was corrected by -11°.

In order to test the frequency response of the hydrophone a number of short, windowed constant frequency pulses were sent. Specifically, pulses were sent at 2 kHz, 5 kHz and 9 kHz. Polar plots showing the attenuation of the beamformed pulses with respect to the omnidirectional channel for the three frequencies were created for angles of arrival of 0° and 60 ° and for two different pattern parameters, $p = 0.5$ and $p = 0.3$.

These plots are shown in Figure 9 and the subcaption indicates the original angle of signal arrival, θ, as well as the corrected angle of arrival, θ_c. The ideal response is plotted with the measured response as a reference to show the close match between the measured and theoretical polar patterns.

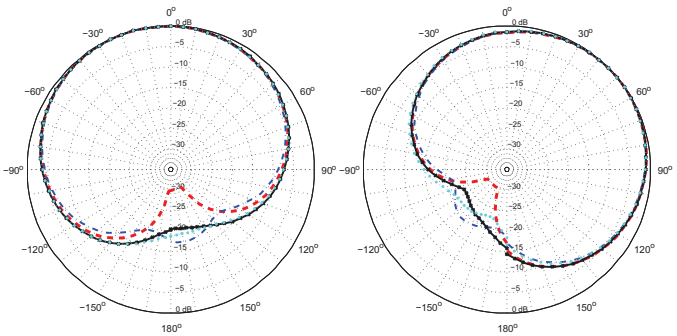

(a) p=0.5, $\theta = 0$, $\theta_c = -11$ (b) p=0.5, $\theta = 60$, $\theta_c = 49$

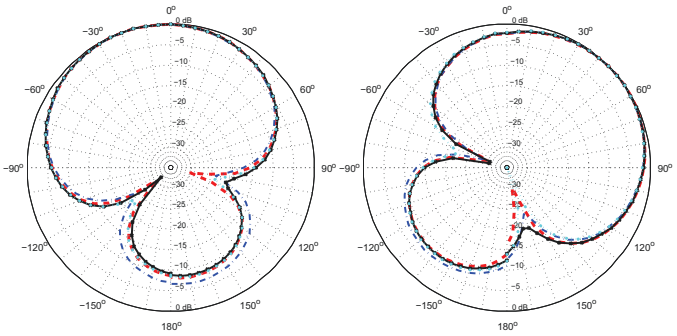

(c) p=0.3, $\theta = 0$, $\theta_c = -11$ (d) p=0.3, $\theta = 60$, $\theta_c = 49$

Fig. 9: Polar patterns measured using short, constant frequency pulses . Red is the ideal response, blue is the measured 2 kHz pattern, black is the measured 5 kHz pattern and turquoise is the measured 9 kHz pattern.

Another test of the directionality of the beamformer was performed by sending a one-second long quadrature phase-shift keyed (QPSK) signal modulated with a maximal length PN sequence with a bandwidth of 6 kHz, from 3 to 9 kHz. The purpose of this experiment was to determine the channel impulse response (CIR) using both the reference, omnidirectional channel and the beamformed data.

To do this the received reference and beamformed data were passed through matched filters and the output of these filters were recorded as the non-directional and directional channel impulse response, respectively. Specifically, the first path arrival at the output of the matched filter was found, and 10 ms of excess delay was recorded after the direct path arrival. Figure 10 contains plots of the output CIR for the reference and beamformed data for different pattern parameters, p. In each plot the reference omnidirectional CIR is shown, and multiple beamformer CIR's are shown with the beamformer steered to different angles, θ.

The CIR's show that the beamformer has the ability to

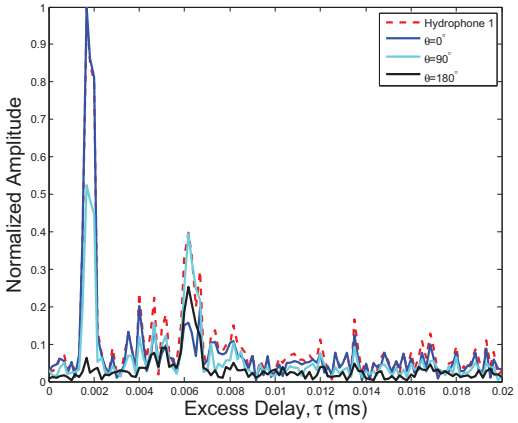

(a) CIR with $p = 0.5$.

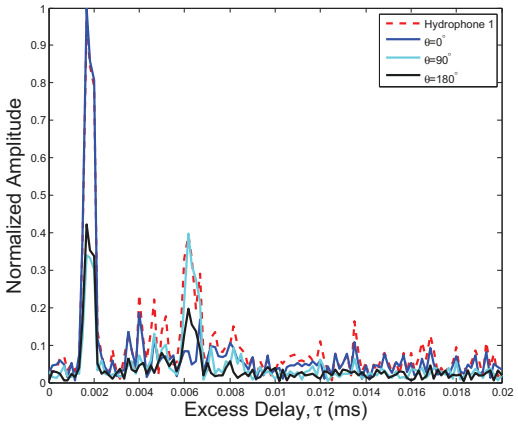

(b) CIR with $p = 0.3$.

Fig. 10: Measured channel impulse responses for omnidirectional and beamformed data steered in different directions, θ.

attenuate and even null out multipath arrivals from different directions. The clearest example of this is the output of beamformed data when $p = 0.5$ and $\theta = 180°$ compared with the reference output in Figure 10a. The direct path, or first path arrival has almost been completely attenuated, indicating that the null of the cardiod pattern, when $p = 0.5$, is pointed at the direct path. While these plots only show a few snapshots of the channel impulse response for the beamformed data from different directions, if the angular resolution is made smaller and the beamformer is swept around it becomes very easy to see the direction of arrival for each multipath component. At that angle output power for the path is maximized.

These experimental results show that the performance of the physical implementation of the planar beamformer using the 5-element hydrophone array closely matches the theoretical performance. Also, no modifications were needed on the recorded signals in order to obtain these results.

V. Conclusion

Soundfield recording techniques present a method for beamforming that requires very few computations once the channels of interest are created. In Section II of this paper the

theory behind soundfield recording was presented with a focus on a first-order, planar beamformer that only requires an omni, cosine and sine channel to produce a beamformed output.

In Section III it was shown that using a discrete 5-element hydrophone array the three required channels for a 2D planar soundfield recording can be produced. A methodology was also presented that explains how the output of the first order cosine and sine channels can be made frequency-flat over a large bandwidth after the discrete derivative is taken with the use of a compensating filter, called the first-order filter.

When this filter is applied to the first-order channels, the beamformer can be made to be extremely wideband. However, care needs to be taken into the acceptable noise floor, as this first-order filter will begin to amplify uncorrelated noise on the hydrophones below a specific frequency, f_{Crit}.

In Section IV, results were presented from experimental trials that show that the theory closely matches the measured results. Specifically, over a frequency band from 2 to 9 kHz the output of the beamformer remained frequency flat with only minor deviations from the ideal pattern. Results were also presented that show that the beamformer can be used to reduce, or even null out, multipath arrivals coming from different directions.

ACKNOWLEDGMENT

The authors would like to thank Mitacs and Turbulent Research for supporting this research. Specifically, thanks to Sebastien Bourdage and Jason Theriault from TR for the time spent on designing and building the TR-Orca, and thanks to my colleague Craig Sheppard for his insight in recording techniques and suggestion to explore Ambisonics.

The authors would also like to thank DRDC Atlantic for the use of their equipment, and Mark Fotheringham for helping us throughout the experimental process.

REFERENCES

[1] R. P. Hodges, *Underwater Acoustics: Analysis, Design and Performance of Sonar*. West Sussex, UK: Wiley, 2010.

[2] M. Gerzon, "Perihoiny: With height sound reproduction," *Journal of the Audio Engineering Society*, vol. 21, no. 1, pp. 2–10, 1973.

[3] P. S. Cotterell, "On the theory of the second order soundfield microphone," Ph.D. dissertation, University of Reading, 2002.

[4] E. Hobson, *The Theory of Spherical and Ellipsoidal Harmonics*. Cambridge University Press, 1931.

[5] A. e. a. Farina, "Ambiophonic principles for the recording and reproduction of surround sound for music," Universit di Parma, Tech. Rep., 2001.

[6] R. Derkx and K. Janse, "Theoretical analysis of a first-order azimuth-steerable superdirective microphone array," *IEEE Transactions on Audio, Speech, and Language Processing*, 2009.

[7] R. Chen, P. Teng, and Y. Yang, "A triple microphone array for surround sound recording."

[8] M. Gerzon, "Ultra directional microphones," *Studio Sound*, 1970.

[9] D. Ernesto, T. Romero, and J. Dolecek, *MATLAB - A Fundamental Tool for Scientific Computing and Engineering Applications*. InTech, 2012, ch. 19 - Digital FIR Hilbert Transformers: Fundamentals and Effecient Design Methods.

[10] W. Liu and S. Weiss, *Wideband Beamforming: Concepts and Techniques*. Wiley, 2010.